Using MERIS on Envisat for land cover mapping in the Netherlands

Clevers, J G P W ; Schaepman, Michael E ; Mücher, C A ; de Wit, A J W ; Zurita-Milla, R ; Bartholomeus, H M

Abstract: This paper describes the results of a feasibility study to test the usefulness of MERIS for land cover mapping. The Netherlands was used as a test site because of its highly fragmented landscape. Results showed that the geometric and radiometric properties of the studied MERIS images of the Netherlands are suitable for land applications. Calculation of principal components and correlation coefficients revealed that the 15 MERIS bands provided a lot of redundant spectral information. For land applications, information came from the visible part of the spectrum on the one hand and from the near-infrared part on the other hand. In addition, the red-edge slope of the reflectance curve (in particular MERIS band 9 at about 708nm) provided supplementary information. The Dutch land use database LGN5 was used as a reference for classifications in this study after aggregation from 25 m to 300 m and recoding to 7 relevant land cover classes. For land cover classification best results in terms of classification accuracies were obtained for the image of 14 July 2003. For the seven land cover classes selected the overall classification accuracy was 67.2%. A multitemporal classification did not improve the overall classification accuracy.

DOI: https://doi.org/10.1080/01431160600821077

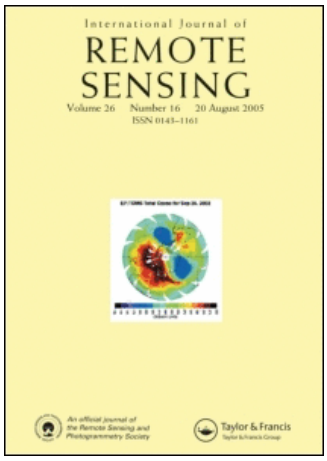

International Journal of Remote Sensing
Publication details, including instructions for authors and subscription information:
http://www.informaworld.com/smpp/title~content=t713722504

Using MERIS on Envisat for land cover mapping in the Netherlands

Online Publication Date: 01 January 2007
To cite this Article: Clevers, J. G. P. W., Schaepman, M. E., Mücher, C. A., de Wit, A. J. W., Zurita-Milla, R. and Bartholomeus, H. M. , (2007) 'Using MERIS on Envisat for land cover mapping in the Netherlands', International Journal of Remote Sensing, 28:3, 637 - 652
To link to this article: DOI: 10.1080/01431160600821077
URL: http://dx.doi.org/10.1080/01431160600821077

International Journal of Remote Sensing
Vol. 28, Nos. 3–4, February 2007, 637–652

Using MERIS on Envisat for land cover mapping in the Netherlands

J. G. P. W. CLEVERS*, M. E. SCHAEPMAN, C. A. MÜCHER, A. J. W. DE WIT, R. ZURITA-MILLA and H. M. BARTHOLOMEUS

Centre for Geo-Information (CGI), Wageningen-UR, P.O. Box 47, NL-6700 AA Wageningen, The Netherlands

This paper describes the results of a feasibility study to test the usefulness of MERIS for land cover mapping. The Netherlands was used as a test site because of its highly fragmented landscape. Results showed that the geometric and radiometric properties of the studied MERIS images of the Netherlands are suitable for land applications. Calculation of principal components and correlation coefficients revealed that the 15 MERIS bands provided a lot of redundant spectral information. For land applications, information came from the visible part of the spectrum on the one hand and from the near-infrared part on the other hand. In addition, the red-edge slope of the reflectance curve (in particular MERIS band 9 at about 708 nm) provided supplementary information. The Dutch land use database LGN5 was used as a reference for classifications in this study after aggregation from 25 m to 300 m and recoding to 7 relevant land cover classes. For land cover classification best results in terms of classification accuracies were obtained for the image of 14 July 2003. For the seven land cover classes selected the overall classification accuracy was 67.2%. A multitemporal classification did not improve the overall classification accuracy.

1. Introduction

Actual and reliable information on land use and land cover (LUC) is required for many application fields at various scale levels. The European landscape is continuously undergoing change caused by a combination of socio-economic and climatic processes. To protect the environment and to ensure sustainable use of natural resources, a wide variety of national and international legal mechanisms have been established, which on their turn have resulted in various environmental monitoring activities. Examples are the EU Habitats Directive (Wils 1994), the EU Common Agricultural Policy (Stoate *et al.* 2001, Olesen and Bindi 2002) and the Kyoto Protocol (Steffen *et al.* 1998). LUC changes play a major role in studying climate change and in particular the global carbon cycle (Houghton *et al.* 1999). Conversion of landscapes, in particular forests, grasslands, wetlands and agricultural lands, contribute significantly to the inherent interannual vegetation dynamics and therefore have an important impact on carbon cycle source and sink estimations and predictions. Moreover, these changes also affect biodiversity. Remotely-sensed data from satellites provide an excellent basis for mapping LUC and LUC changes (Gutman *et al.* 2004).

On the one hand, global datasets derived from coarse resolution sensors provide information on land cover globally. In the US, global land cover products have been

*Corresponding author. Email: jan.clevers@wur.nl

International Journal of Remote Sensing
ISSN 0143-1161 print/ISSN 1366-5901 online
http://www.tandf.co.uk/journals
DOI: 10.1080/01431160600821077

derived using time series with 1 km data obtained from the National Oceanic and Atmospheric Administration's (NOAA) Advanced Very High Resolution Radiometer (AVHRR) (Hansen *et al.* 2000, Loveland *et al.* 2000). In Europe, 1 km data from the Vegetation instrument (VGT), on board the Système Probatoire de l'Observation de la Terre (SPOT)-4, have been used for producing land cover products (Bartalev *et al.* 2003). Recently, a 1 km land cover map has been compiled using a time series of data from the Moderate Resolution Imaging Spectroradiometer (MODIS) on the Terra platform (Friedl *et al.* 2002). This coarse scale imagery is limiting the use for monitoring purposes due to the finer scale at which most land cover changes take place in Europe (Mücher *et al.* 2000). Still these sub-kilometre scale changes are critical for monitoring changes in, e.g., sinks and sources of the carbon cycle or changes in biodiversity.

On the other hand, many detailed studies at the regional and landscape scale at spatial resolutions between 10 m and 30 m have been performed using the Thematic Mapper (TM) aboard the Landsat satellites (Cohen and Goward 2004), the multispectral imager (denoted by XS) aboard the SPOT satellites (Bartholome and Belward 2005) or the Advanced Spaceborne Thermal Emission and Reflector Radiometer (ASTER) aboard the Terra platform (Marcal *et al.* 2005). The use of such data is usually not appropriate at the continental scale due to their limited spatial extent and low revisit time. The gap between fine and coarse resolution sensors may be filled with imagery at spatial resolutions of 250 m using MODIS (Zhan *et al.* 2002) or 300 m using the Medium Resolution Imaging Spectrometer (MERIS) (Rast *et al.* 1999). The MODIS Science Team stated that a detection method for land cover change should better be based on MODIS 250 m data than on MODIS 500 m or 1 km data (Zhan *et al.* 2002), since relevant land cover changes induced by human activities occur at typical spatial scales in the order of 250 m (Townshend and Justice 1988).

The enhanced spatial, spectral, radiometric and geometric quality of MODIS and MERIS data provides a greatly improved basis for mapping and monitoring land cover as compared to AVHRR data (Verstraete *et al.* 1999). In this paper our primary objective was to study the information content of MERIS full resolution images over land, and to investigate whether such images can be used to discriminate the major land cover types relevant for a highly fragmented landscape. Monotemporal and multitemporal classifications were compared. As a feasibility study towards the use of MERIS for land cover mapping, we were focussing on the Netherlands as an example of a densely populated Western European region. Its landscape is exemplary for general fragmentation issues at the (Western) European scale (Faludi 2004).

2. Material and methods

2.1 *MERIS data*

MERIS is one of the payload components of the European Space Agency's (ESA) environmental research satellite Envisat, launched in March 2002. MERIS is a 15 band imaging spectrometer. It is designed to acquire data at variable bandwidth of 1.25 to 30 nm over the spectral range of 390–1040 nm (Rast *et al.* 1999). Specifications of the spectral bands are given in table 1 (as provided in the metadata of the used images). Data are acquired at 300 m full resolution (FR) mode or 1200 m reduced resolution (RR) mode over land.

Table 1. The 15 spectral bands of the MERIS images.

Band nr.	Band centre (nm)	Bandwidth (nm)
1	412.5	9.9
2	442.4	10.0
3	489.7	10.0
4	509.7	10.0
5	559.6	10.0
6	619.6	10.0
7	664.6	10.0
8	680.9	7.5
9	708.4	10.0
10	753.5	7.5
11	761.6	3.7
12	778.5	15.0
13	864.8	20.0
14	884.8	10.0
15	899.8	10.0

For this study four FR MERIS images for the Netherlands from 2003 were used. Cloud free images from 16 April and 14 July 2003, were available. Images from 18 February and 16 June 2003, showed considerable cloud cover over the northern part of the country, but the southern part was cloudless. The images are depicted in figure 1. The data comprised geocoded top of atmosphere (TOA) radiances [$Wsr^{-1}m^{-2}\mu m^{-1}$] (MERIS Level 1b product). Detailed information on the recorded images is given in table 2. First, the geocoded data were converted using an affine transformation to the Dutch national coordinate system (RD), which is a stereographic projection. The transformation was done using the latitude and longitude coordinates of nine tie-points, defined by the corner points of the four image quadrants. Cubic convolution was used as a resampling procedure. For 2003, the reported geolocation accuracy of MERIS data was about 209 m along-track and about 295 m across-track (Goryl and Saunier 2004). These deviations were taken into account in the current study. Subsequently, a mask was applied in order to create a data set only covering the Netherlands. Finally, the TOA radiances were converted to TOA reflectances (planetary reflectances) by using the information on TOA solar irradiance [$Wm^{-2}\mu m^{-1}$] and solar angle (ϑ_s) according to equation (1).

$$\rho_{TOA} = \frac{\pi L_{TOA}}{E_i \cos\vartheta_s} \tag{1}$$

where ρ is reflectance, TOA is Top of Atmosphere, L is radiance measured at the sensor, E_i is solar irradiance.

Due to the resemblance of planetary reflectance to ground reflectance, it will allow a better interpretation of the satellite measurements without the need of a full atmospheric correction. Moreover, it will minimize the impact of solar illumination differences for a multitemporal comparison (as done in figure 4).

2.2 *Land cover information*

As a reference database, the Dutch land use database (LGN) was used. It is a geographical database that describes the land use in the Netherlands. The database uses a grid structure with a cell size of 25 metres; the application scale is about 1:50.000. Today, the LGN database contains 39 land use classes covering urban

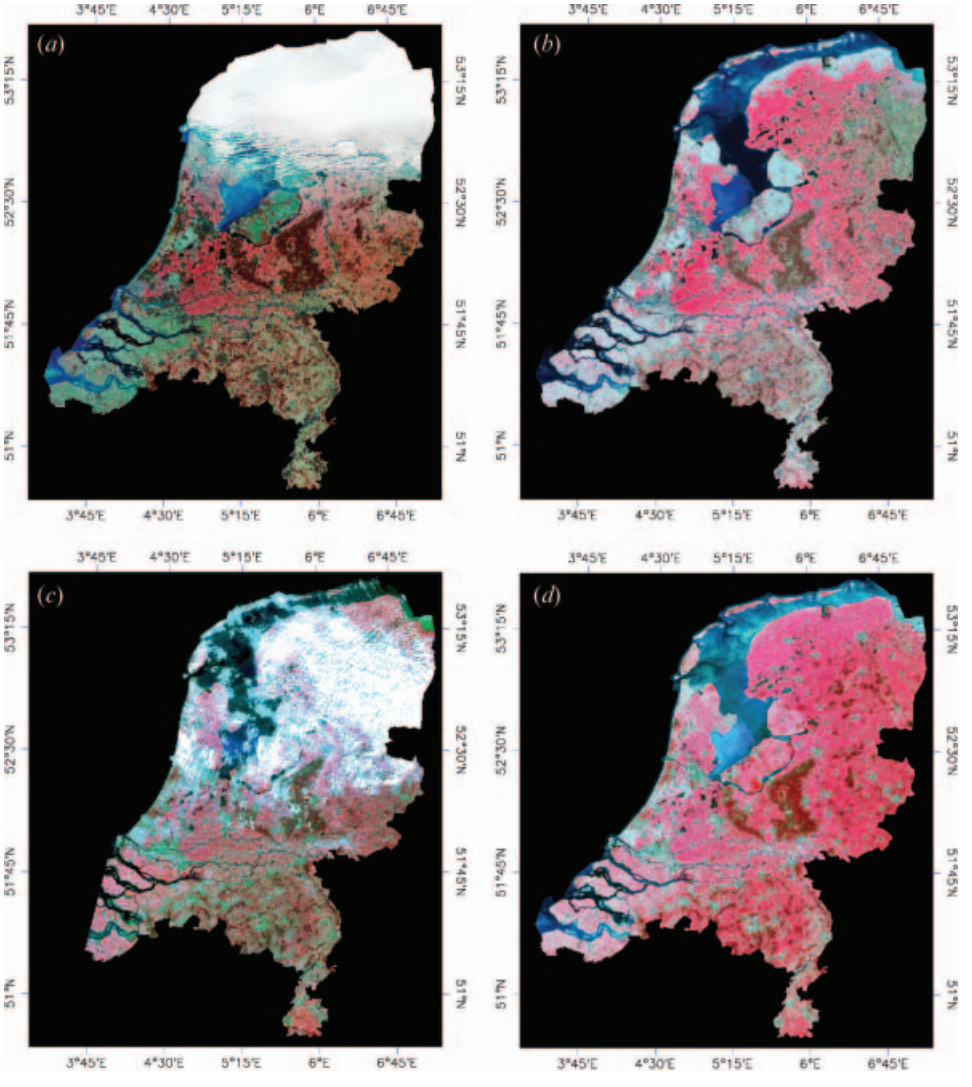

Figure 1. MERIS full resolution image of 18 February (*a*), 16 April (*b*), 16 June (*c*) and 14 July (*d*) 2003, for the Netherlands. Bands 14, 7 and 5 are depicted in RGB.

areas, water, forest, various agricultural crops and artificial, semi-natural and natural land cover classes. For this study the latest available version (LGN5), based on satellite data of 2003 and 2004, was used. LGN is based on a stratified multitemporal classification of satellite imagery and integration of ancillary data.

Table 2. Some characteristics of the MERIS images used in this study.

Recording date	Processing level	Recording time (UTC)	Solar angle
18 Feb 2003	1B	10:19	67.1
16 Apr 2003	1B	10:28	44.4
16 Jun 2003	1B	10:11	33.1
14 Jul 2003	1B	10:30	33.5

The overall classification accuracy of LGN at class level is 85–90%, which is obtained by applying a per-field classification for the agricultural crops (De Wit and Clevers 2004).

The International Geosphere-Biosphere Programme (IGBP) has developed a list of classes that are relevant for global land cover changes (Hansen *et al*. 2000). Out of the 17 land cover classes based on the IGBP DISCover land cover legend (Loveland and Belward 1997), the following classes are relevant for the Netherlands as test site: grassland, arable land, coniferous forest, deciduous forest, natural vegetation (e.g., heather), built-up areas and water bodies.

The 39 classes of the LGN database were recoded into the mentioned 7 land cover classes using the LGN legend structure. Subsequently, the grid was spatially aggregated to 300 metres assigning the most frequently occurring (majority) class as label. The resulting image is shown in figure 2. In the current study, this aggregated database was used as a reference. One has to realize that in principle most pixels are mixed pixels, originating from various different land cover classes (for estimation of pure pixels in LGN, refer to Zurita-Milla (2007, this issue)). Moreover, the class 'arable land' originates from many different crop types (with different spectral and temporal signatures). Table 3 shows the frequency distribution of the 7 classes.

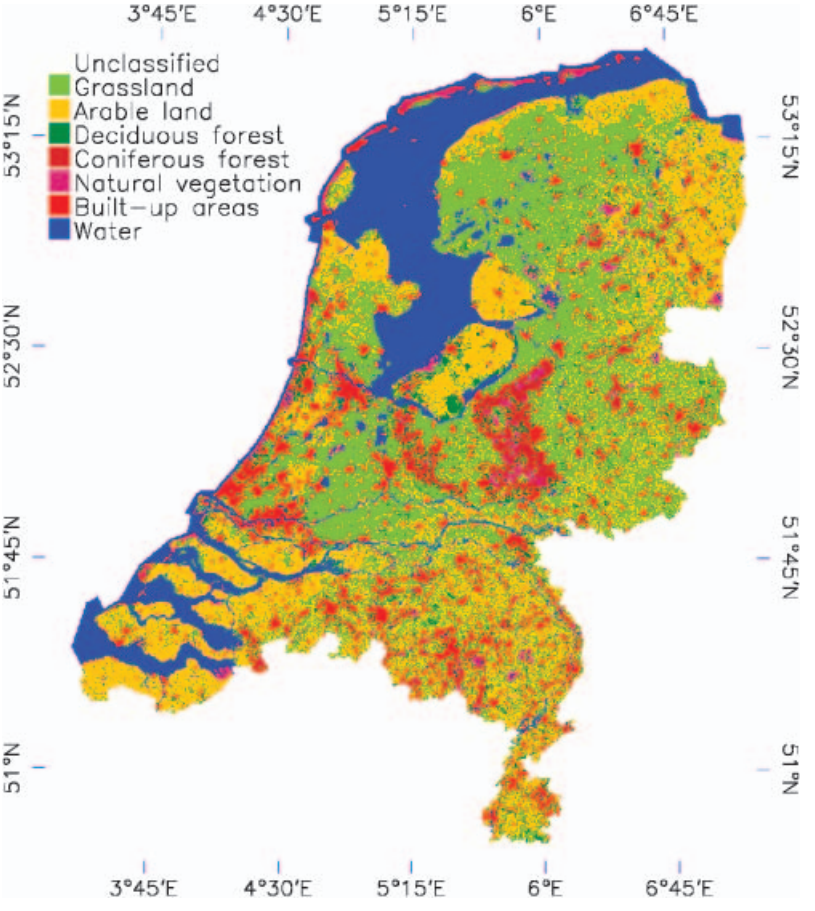

Figure 2. The Dutch land use database aggregated to 7 classes and 300 m pixel size.

Table 3. Main land cover types in the Netherlands (derived from LGN5).

Land cover	% of total area
Grassland	37.3
Arable land	24.2
Deciduous forest	3.0
Coniferous forest	4.9
Natural vegetation	1.7
Built-up areas	10.7
Water	18.2

2.3 *Image analysis*

First, the geometric properties of the MERIS images were studied visually and subsequently the RD-coordinates of ground control points were compared with those of the LGN database. In order to study the information content of the MERIS images, principal components and between-band correlation coefficients were calculated. MERIS bands 1 and 2 were omitted from the analysis due to the high atmospheric scattering in the blue part of the spectrum. In the near-infrared (NIR) the spectral signature showed a dip at about 762 nm (band 11) due to absorption by oxygen in the atmosphere (Heidinger and Stephens 2000). This band was not used any further in this study. Finally, band 15 at 900 nm was not used in this study because its purpose is determining the water vapour in the atmosphere (Bennartz and Fischer 2001). As a result, the spectral range from 490 nm up to 885 nm with 11 bands was used. Subsequently, training samples for the main land cover classes were collected using the aggregated Dutch land cover database LGN as a reference. Per class three polygons of about 100 pixels each were identified in areas homogeneous for the particular class, reducing the effect of mixed pixels as much as possible at the training stage. Thereafter the spectral and temporal signatures of the main land cover classes were studied. Finally, a minimum-distance-to-means and a maximum likelihood supervised classification were performed, as these are the most common classification procedures. For the February and June images clouds were included as a separate class in the training stage (the cloud flag assigned by the MERIS processor did not properly indicate all the clouded pixels and was therefore not used in this study). The classification accuracies were evaluated based on the error matrices using the whole aggregated land cover database as a reference (and excluding the class "clouds"). This included the training pixels, but since their number was small relative to the size of the whole database (less than 1%), their influence on the overall classification accuracies is negligible. In addition, the Kappa coefficient was calculated as a measure for the agreement between the classified and reference data corrected for chance agreement (Congalton and Green 1999).

Using the April and July cloudless images a multitemporal classification could be applied for the whole test area. The first two principal components of each date were used for this. Results were compared with the monotemporal classification results.

3. Results

3.1 *Image characteristics*

First, geometric properties of all four images were studied. Latitude and longitude coordinates for every pixel were determined by using only 9 tie points (corners of the

image quadrants). Resulting pixel coordinates were the same as the ones obtained using the BEAM software (Brockmann 2004) using all tie points. Subsequently, the geographic projection was reprojected into the stereographic projection of the Dutch RD coordinate system. No external information was used for this transformation. Visually the resulting images (figure 1) matched the LGN database well (e.g., figure 3). A geometric registration with the LGN database using a large number of GCPs showed that the MERIS images should be shifted one pixel to the left (x direction) and one pixel up (y direction) in order to get an optimal fit. Table 4 provides the average translation errors in terms of root-mean-square (RMS) error. The shift of the MERIS pixel appeared to be a systematic one for all MERIS images analysed and can be fully explained by the geolocation inaccuracy of MERIS FR level 1B products in 2003 for the Northern hemisphere as reported by the Product Control Facility of ESRIN (Goryl and Saunier 2004).

The principal component analysis showed that more than 99% of all information was captured in the first two components for all dates (cf. table 5). The first principal component had particularly high positive loadings for the MERIS bands 10 till 14, meaning the bands in the NIR region, whereas the loadings of the other bands were small. Component 2 had high loadings for bands 3 till 9, representing the visible region, whereas the loadings of the other bands were small. Component 3 mainly

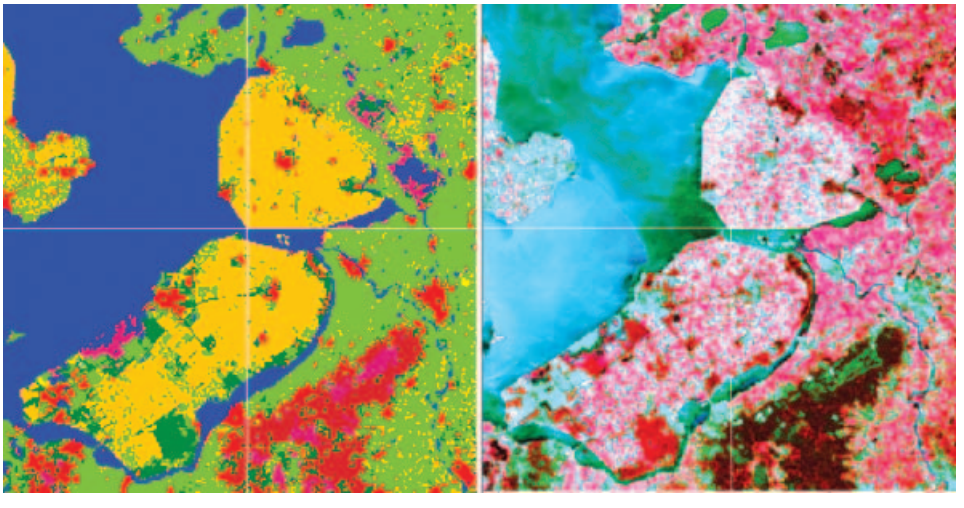

Figure 3. Comparison of the geometry of the MERIS image of 14 July 2003, to the right and the aggregated LGN database to the left.

Table 4. Root-mean-square (RMS) errors (in m) of the comparison of the georeferenced MERIS images using the information of only 9 image tie points and the Dutch RD coordinate system.

Recording date	RMS error X coord.	RMS error Y coord.	RMS error total
18 Feb 2003	250	313	400
16 Apr 2003	286	152	324
16 Jun 2003	255	226	341
14 Jul 2003	267	353	442

Table 5. Example of results of a principal component analysis (MERIS image of 14 July 2003).

Principal component	Accounted variance (%)	Cumulative variance (%)
1	95.68	95.68
2	4.04	99.71
3	0.16	99.87
4	0.06	99.93
5	0.05	99.98
6	0.01	99.99
7	0.01	100.0
8	0.00	100.0
9	0.00	100.0
10	0.00	100.0
11	0.00	100.0

exhibited the contrast between band 9 and a number of the other bands (varying for the various images), showing some specific information in the red-edge region.

Table 6 shows an example of the correlation coefficients between the individual spectral bands of MERIS over land. First of all, it can be observed that bands 3 till 8 (all in the visible) were strongly correlated. Subsequently, table 6 shows that also bands 10 till 14 (in the NIR) were strongly correlated. Band 9 at the red-edge slope (at about 708 nm) showed a deviating behaviour as it was moderately correlated with the visible bands as well as with the NIR bands. It took an intermediate position, making it a particularly interesting band of the MERIS sensor. Similar results were obtained for the other images (Clevers *et al*. 2004).

3.2 *Spectral signatures*

Figure 4 depicts the spectral signatures of the main land cover classes as derived from the MERIS training samples for the different images. The general shape of the TOA reflectances corresponded to typical spectra of the respective classes. The first few bands showed a relatively high reflectance due to atmospheric scattering. Vegetation classes showed a steep slope between the red and NIR reflectance.

Table 6. Correlation matrix for a subset of the MERIS image of 14 July 2003.

band	3	4	5	6	7	8	9	10	12	13	14
(nm)	489.7	509.7	559.6	619.6	664.6	680.9	708.4	753.5	778.5	864.8	884.8
3	1										
4	0.996	1									
5	0.911	0.939	1								
6	0.938	0.956	0.960	1							
7	0.925	0.939	0.925	0.992	1						
8	0.916	0.930	0.917	0.988	0.999	1					
9	0.356	0.409	0.648	0.606	0.594	0.606	1				
10	−0.309	−0.262	0.026	−0.085	−0.101	−0.083	0.701	1			
12	−0.332	−0.285	0.002	−0.108	−0.123	−0.106	0.683	0.999	1		
13	−0.346	−0.299	−0.013	−0.118	−0.131	−0.113	0.683	0.997	0.998	1	
14	−0.347	−0.300	−0.014	−0.118	−0.131	−0.113	0.684	0.997	0.998	0.999	1

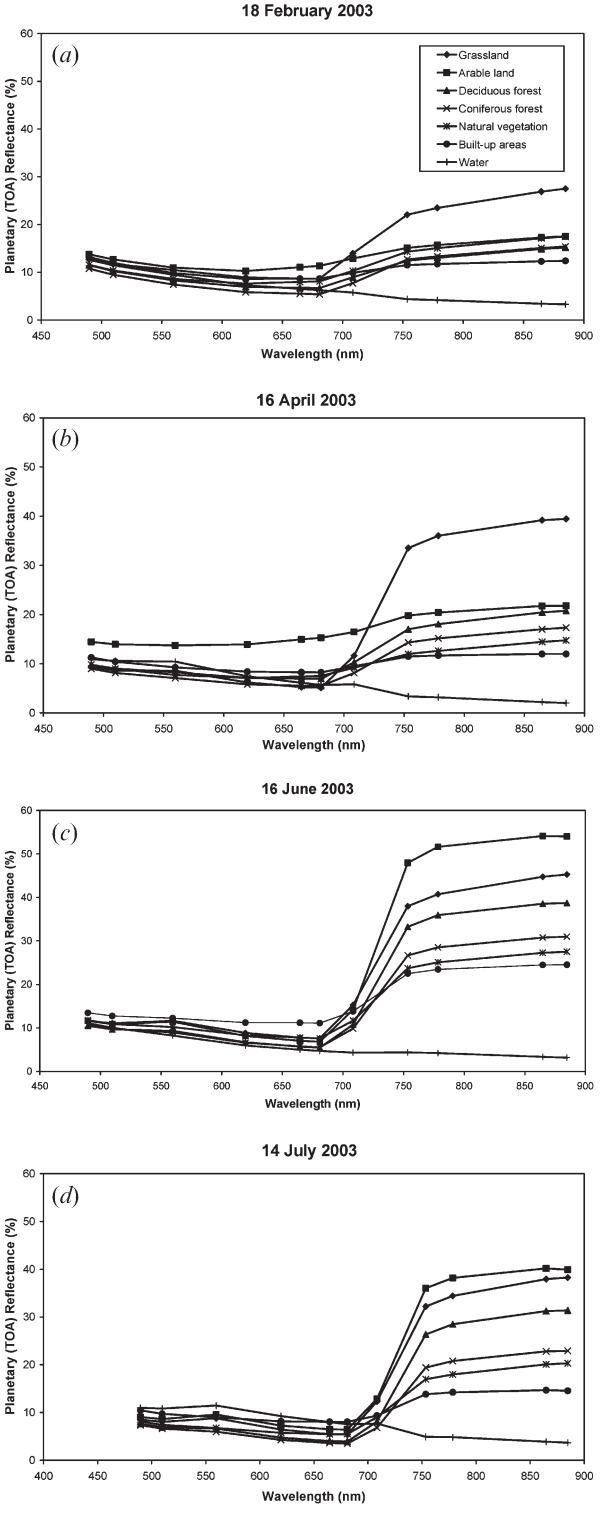

Figure 4. Spectral signatures for the main land cover types derived from the MERIS image of 18 February (*a*), 16 April (*b*), 16 June (*c*) and 14 July (*d*), 2003.

Spectral signatures for 18 February (figure 4(*a*)) only exhibited a limited dynamic range. Water had a low reflectance in the NIR and grassland had a relatively high reflectance in the NIR. The other signatures were close to each other and when taking the standard deviation of the observations into account (data not shown) the conclusion must be that the signatures showed significant overlap. Conditions in February were quite wet, explaining the low reflectance values for most classes. February was too early in the growing season to differentiate most classes of interest. In addition, the particular image of 2003 was only partly usable due to cloud cover.

Spectral signatures for 16 April (figure 4(*b*)) showed a clear vegetation spectrum for grassland. On the other hand, arable land still showed a flat reflectance signature as to be expected for a barren land signature (albeit at a higher value than in February). The signatures for deciduous forest, coniferous forest and natural vegetation were quite similar, showing a vegetation spectrum (low reflectance in the visible part and a higher reflectance in the NIR). Built-up areas and water showed similar spectra as in February.

The spectral signature of grassland for 16 June (figure 4(*c*)) was similar to the one in April (although it indicated a further increase in biomass). However, the signature

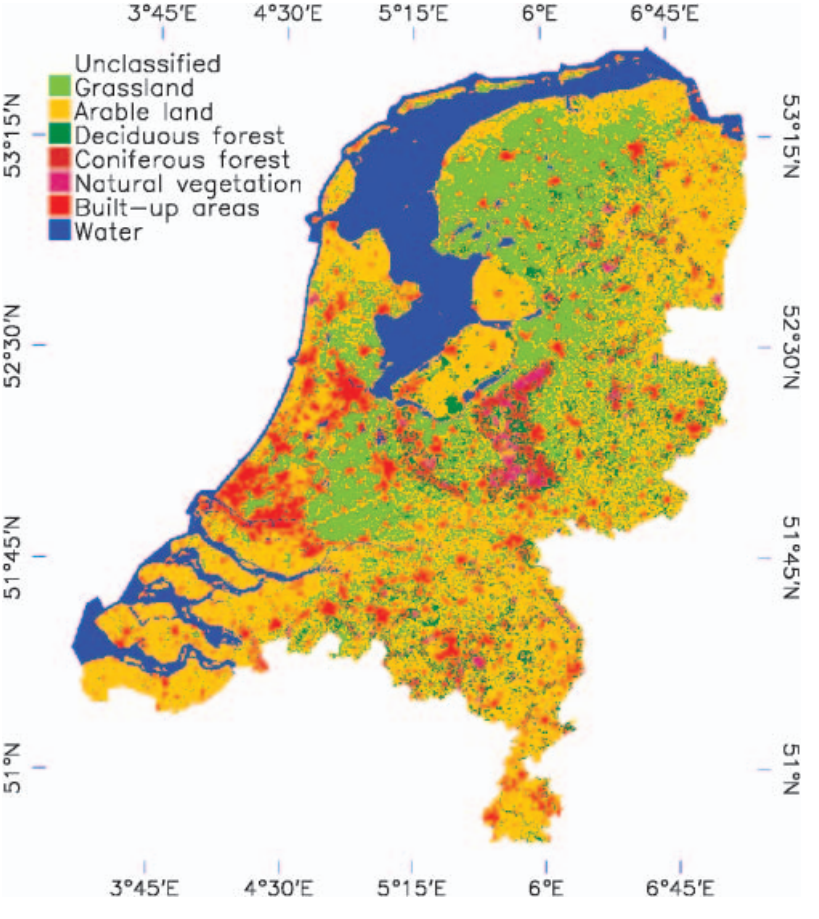

Figure 5. Result of the maximum likelihood classification based on the MERIS image of 14 July 2003.

of arable land changed to that of a clear vegetation spectrum and indicated an even larger amount of biomass than that of grassland. Also the signature of deciduous forest changed to a typical vegetation spectrum. The same is true for the spectra of coniferous forests and natural vegetation. Their reflectance in the NIR part is relatively low due to the vegetation properties (type and structure). The spectrum for built-up areas showed some influence of vegetation in the signature, which may be expected at this spatial scale. Finally, the spectrum of water was comparable to that of the previous dates.

The signature of grassland for 14 July (figure 4(*d*)) was similar to the one for June 16th. The signature of arable land approached that of grassland indicating some crop maturing for the July data. Overall the TOA reflectances were a bit lower for the July image than for the June image. This might be caused by atmospheric influences.

3.3 *Classification*

Classification accuracies were determined by using the whole land cover database (figure 2) as a reference. The maximum likelihood classification rule gave better results than the minimum distance to means classification (data not shown). Table 7 shows the results for the main land cover classes for 14 July 2003. This was an image in the middle of the growing season without any cloud cover. The overall accuracy was 67.2%. The Kappa coefficient was 0.574. Table 8 provides the complete error matrix. This table shows that the arable land in the classification result originated not only from the arable land in the reference map, but actually from all other classes as well. The heterogeneous nature of arable land, resulting from the complex patterns and the variations in growth of the various crops, makes it impossible to map the arable land class accurately at the MERIS scale level (300 m) using computer-assisted image classification methods. More than half of the classified arable land pixels originated from other land cover classes. The grassland was in particular confused with the arable land. In addition, the coniferous forest was mainly confused with the deciduous forest and to a lesser extent with natural vegetation (in addition again to the confusion with the arable land). The final result is that the total area of arable land was severely overestimated (by 82%), while the total area of grassland and coniferous forest was underestimated when looking at the classification result (by 41% and 58%, respectively).

The maximum likelihood classification for the cloudless image of 16 April, 2003, yielded an overall accuracy of 62.3% (results not shown), which was slightly less than the one for the July acquisition. Although it was concluded from the spectral signatures (figure 4(*b*)) that grassland could be well differentiated in April, the

Table 7. Classification results for the MERIS image of 14 July 2003.

Class	Producer's accuracy (%)	User's accuracy (%)
Grassland	52.9	89.5
Arable land	89.7	49.3
Deciduous forest	47.8	26.1
Coniferous forest	38.9	91.9
Natural vegetation	34.9	50.0
Built-up areas	63.6	69.0
Water	82.5	98.2
	Overall Accuracy=67.2%	Kappa coefficient=0.574

Table 8. Error matrix of the classification for the MERIS image of 14 July 2003. GL=grassland; AL=arable land; DF=deciduous forest; CF=coniferous forest; NV=natural vegetation; BU=built-up areas; W=water; PA=producer's accuracy; UA=user's accuracy.

		Reference map (LGN5)							
		GL	AL	DF	CF	NV	BU	W	UA
Classification result	GL	**90839**	7218	618	109	613	1307	742	0.895
	AL	65033	**99652**	5363	3613	3123	15234	10274	0.493
	DF	7871	1826	**6546**	7126	842	694	144	0.261
	CF	99	27	493	**8671**	108	19	20	0.919
	NV	495	52	100	1807	**2684**	117	110	0.500
	BU	6906	2263	532	970	245	**31558**	3254	0.690
	W	368	81	39	2	83	665	**68713**	0.982
	PA	0.529	0.897	0.478	0.389	0.349	0.636	0.825	

classification result for grassland was a bit disappointing. Variation in biomass for the various grassland pixels yielded a large variation for the spectral signatures. We could not clearly identify any class that was classified much better (user's and producer's accuracy) as compared to the July image.

Due to partial cloud cover, the error matrix for 16 June 2003, could only be ascertained for the southern part of the country. The overall classification accuracy was slightly less than the previous ones (59.1%). Of course some remaining influence of clouds in the classified pixels may affect these results.

For 18 February 2003, again only the southern part of the country could be used. As expected from the spectral signatures (figure 4a), the classification results were quite poor. The overall classification accuracy was 43.2%.

Finally, it was tested whether a multitemporal classification could improve the results of the monotemporal classifications. The first two principal components for the cloud free April and July images were combined therefore. Results for the maximum likelihood classification are given in table 9. The overall classification accuracy was 64.3%. Results were not better than for the July image alone.

4. Discussion and conclusions

This study showed that the national coordinate system of the Netherlands could easily be reprojected to the MERIS images by using the latitude and longitude coordinates that are provided by MERIS metadata for nine tie points in the image.

Table 9. Classification results after combining the first two principal components of the MERIS image of 16 April and 14 July 2003.

Class	Producer's accuracy (%)	User's accuracy (%)
Grassland	56.0	87.5
Arable land	77.7	55.0
Deciduous forest	58.2	16.7
Coniferous forest	46.7	90.9
Natural vegetation	41.2	16.6
Built-up areas	57.2	55.8
Water	75.4	99.5
	Overall Accuracy=64.3%	Kappa coefficient=0.545

The remaining error was in the order of one pixel. Using the TOA solar irradiance and the solar angle provided by MERIS metadata for the time of image recording as part of the image files one could easily derive spectral signatures in terms of TOA reflectance. The resulting spectral signatures showed that MERIS has the potential to differentiate the major land cover types in the Netherlands.

Calculation of principal components and correlation coefficients revealed that MERIS provides information over land mainly related to the visible part of the spectrum on the one hand and the NIR part on the other hand. This means that MERIS has redundant information in its 15 spectral bands for land applications. However, spectral bands at the red-edge slope of the reflectance curve (in particular MERIS band 9 at about 708 nm) provided additional information, which may be an important innovative feature of the MERIS sensor for vegetation studies. Future studies will also look at deriving continuous information from MERIS images, whereby the red-edge position will receive special attention. In this respect, attention will also focus on the use of level 2 MERIS products. The development of the MERIS terrestrial chlorophyll index (MTCI) is one of the more recent products (Dash and Curran 2004).

Good results were already obtained with a monotemporal classification of the land use of the Netherlands. Best results were obtained for the MERIS image of 14 July 2003. For 7 classes the overall classification accuracy was 67.2%. It should be stressed that MERIS pixels at 300 m most often are mixed pixels consisting of various land cover types (even for the aggregated classes used in this study) for a highly fragmented landscape as studied in this paper. Not only is a MERIS pixel often heterogeneous, also the class definitions used will impose heterogeneous classes in some cases. Results show, for instance, that the user's accuracy of arable land was quite low. The arable land class is such a very heterogeneous class due to the many different crop types, resulting also in heterogeneous training samples for arable land at the MERIS scale level. As a result, numerous pixels from other classes were assigned the label arable land, which resulted in a significant overestimation of the arable land area in the Netherlands. Agriculture was recognized as being by far the most problematic class in global land cover mapping contexts (Hansen *et al.* 2000, Loveland *et al.* 2000). As such, a classification accuracy of 67.2% at this scale level can be considered a good result. Even an unsupervised classification into a large number of classes and a subsequent assignment of labels did not give a significantly better result (Clevers *et al.* 2005).

Further research will focus on the extension to other regions in Europe and the use of level 2 MERIS products. Since it is evident that MERIS pixels often are mixed pixels comprising various land cover types, sub-pixel analysis techniques must be explored in future.

A major disadvantage of using MERIS for land cover classifications is the lack of a short-wave infrared (SWIR) spectral band. The SWIR band available in, e.g., SPOT-Vegetation data offers additional information that can improve the discrimination of vegetation cover types (Latifovic *et al.* 2004). Sato and Tateishi (2004) showed that the SWIR is particularly important for discriminating barren or sparsely vegetated areas.

Further improvement of the classification results can be obtained by using a time-series of e.g. monthly remote sensing images, by making full use of the phenological variation of the vegetation throughout the year (Verhoef *et al.* 1996). Therefore, MERIS products like maximum value composites of a vegetation index over a

certain period of time (e.g. decade or month) have to be developed, as is e.g. provided for MODIS data. As soon as such products will be provided for MERIS, its full potential for land cover monitoring can be exploited. To conclude, MERIS is a relevant sensor for land applications with features not yet provided by other satellite sensors (Curran and Steele 2005).

Acknowledgements

This work was performed in the framework of ESA project AO 508. ESA is acknowledged for providing the MERIS data.

References

Bartalev, S.A., Belward, A.S., Erchov, D.V. and Isaev, A.S., 2003, A new SPOT4-VEGETATION derived land cover map of Northern Eurasia. *International Journal of Remote Sensing*, **24**, pp. 1977–1982.

Bartholome, E. and Belward, A.S., 2005, GLC2000: a new approach to global land cover mapping from Earth observation data. *International Journal of Remote Sensing*, **26**, pp. 1959–1977.

Bennartz, R. and Fischer, J., 2001, Retrieval of columnar water vapour over land from backscattered solar radiation using the Medium Resolution Imaging Spectrometer. *Remote Sensing of Environment*, **78**, pp. 274–283.

Brockmann, C., 2004, Demonstration of the BEAM software – A tutorial for making best use of VISAT. In MERIS User Workshop, 10–13 November 2003, Frascati, Italy (Noordwijk: ESA), p. 4.

Clevers, J.G.P.W., Bartholomeus, H.M., Mücher, C.A. and De Wit, A.J.W., 2004, Use of MERIS data for land cover mapping in the Netherlands. In MERIS User Workshop, 10–13 November 2003, Frascati, Italy (Noordwijk: ESA), p. 6.

Clevers, J.G.P.W., Zurita Milla, R., Schaepman, M.E. and Bartholomeus, H.M., 2005, Using MERIS on Envisat for land cover mapping. In Proceedings of the 2004 Envisat & ERS Symposium, 6–10 September 2004, Salzburg, Austria (Noordwijk: ESA), p. 10.

Cohen, W.B. and Goward, S.N., 2004, Landsat's role in ecological applications of remote sensing. *BioScience*, **54**, pp. 535–545.

Congalton, R.G. and Green, K., 1999, Assessing the accuracy of remotely sensed data. Principles and practices. (Boca Raton, FL: Lewis Publishers).

Curran, P.J. and Steele, C.M., 2005, MERIS: the re-branding of an ocean sensor. *International Journal of Remote Sensing*, **26**, pp. 1781–1798.

Dash, J. and Curran, P.J., 2004, The MERIS terrestrial chlorophyll index. *International Journal of Remote Sensing*, **25**, pp. 5403–5413.

De Wit, A.J.W. and Clevers, J., 2004, Efficiency and accuracy of per-field classification for operational crop mapping. *International Journal of Remote Sensing*, **25**, pp. 4091–4112.

Faludi, A., 2004, The European spatial development perspective and North-west Europe: Application and the future. *European Planning Studies*, **12**, pp. 391–408.

Friedl, M.A., McIver, D.K., Hodges, J.C.F., Zhang, X.Y., Muchoney, D., Strahler, A.H., Woodcock, C.E., Gopal, S., Schneider, A., Cooper, A., Baccini, A., Gao, F. and Schaaf, C., 2002, Global land cover mapping from MODIS: algorithms and early results. *Remote Sensing of Environment*, **83**, pp. 287–302.

Goryl, P. and Saunier, S., 2004, MERIS absolute geolocation status. In MERIS Cyclic Report, edited by ESRIN-PCF (Frascati: ESRIN), p. 10.

Gutman, G., Janetos, A.C., Justice, C.O., Moran, E.F., Mustard, J.F., Rindfuss, R.R., Skole, D., Ii, B.L.T. and Cochrane, M.A., 2004, Land Change Science: Observing,

Monitoring and Understanding Trajectories of Change on the Earth's Surface (Berlin: Springer-Verlag).

HANSEN, M.C., DEFRIES, R.S., TOWNSHEND, J.R.G. and SOHLBERG, R., 2000, Global land cover classification at 1km spatial resolution using a classification tree approach. *International Journal of Remote Sensing*, **21**, pp. 1331–1364.

HEIDINGER, A.K. and STEPHENS, G.L., 2000, Molecular line absorption in a scattering atmosphere. Part II: Application to remote sensing in the O-2 A band. *Journal of the Atmospheric Sciences*, **57**, pp. 1615–1634.

HOUGHTON, R.A., HACKLER, J.L. and LAWRENCE, K.T., 1999, The US carbon budget: Contributions from land-use change. *Science*, **285**, pp. 574–578.

LATIFOVIC, R., ZHU, Z.L., CIHLAR, J., GIRI, C. and OLTHOF, I., 2004, Land cover mapping of north and central America – Global Land Cover 2000. *Remote Sensing of Environment*, **89**, pp. 116–127.

LOVELAND, T.R. and BELWARD, A.S., 1997, The IGBP-DIS global 1 km land cover data set, DISCover: first results. *International Journal of Remote Sensing*, **18**, pp. 3291–3295.

LOVELAND, T.R., REED, B.C., BROWN, J.F., OHLEN, D.O., ZHU, Z., YANG, L. and MERCHANT, J.W., 2000, Development of a global land cover characteristics database and IGBP DISCover from 1 km AVHRR data. *International Journal of Remote Sensing*, **21**, pp. 1303–1330.

MARCAL, A.R.S., BORGES, J.S., GOMES, J.A. and DA COSTA, J.F.P., 2005, Land cover update by supervised classification of segmented ASTER images. *International Journal of Remote Sensing*, **26**, pp. 1347–1362.

MÜCHER, C.A., STEINNOCHER, K.T., KRESSLER, F.P. and HEUNKS, C., 2000, Land cover characterization and change detection for environmental monitoring of pan-Europe. *International Journal of Remote Sensing*, **21**, pp. 1159–1181.

OLESEN, J.E. and BINDI, M., 2002, Consequences of climate change for European agricultural productivity, land use and policy. *European Journal of Agronomy*, **16**, pp. 239–262.

RAST, M., BEZY, J.L. and BRUZZI, S., 1999, The ESA Medium Resolution Imaging Spectrometer MERIS – a review of the instrument and its mission. *International Journal of Remote Sensing*, **20**, pp. 1681–1702.

SATO, H.P. and TATEISHI, R., 2004, Land cover classification in SE Asia using near and short wave infrared bands. *International Journal of Remote Sensing*, **25**, pp. 2821–2832.

STEFFEN, W., NOBLE, I., CANADELL, J., APPS, M., SCHULZE, E.D., JARVIS, P.G., BALDOCCHI, D., CIAIS, P., CRAMER, W., EHLERINGER, J., FARQUHAR, G., FIELD, C.B., GHAZI, A., GIFFORD, R., HEIMANN, M., HOUGHTON, R., KABAT, P., KORNER, C., LAMBIN, E., LINDER, S., MOONEY, H.A., MURDIYARSO, D., POST, W.M., PRENTICE, I.C., RAUPACH, M.R., SCHIMEL, D.S., SHVIDENKO, A. and VALENTINI, R., 1998, The terrestrial carbon cycle: Implications for the Kyoto Protocol. *Science*, **280**, pp. 1393–1394.

STOATE, C., BOATMAN, N.D., BORRALHO, R.J., CARVALHO, C.R., DE SNOO, G.R. and EDEN, P., 2001, Ecological impacts of arable intensification in Europe. *Journal of Environmental Management*, **63**, pp. 337–365.

TOWNSHEND, J.R.G. and JUSTICE, C.O., 1988, Selecting the Spatial-Resolution of Satellite Sensors Required for Global Monitoring of Land Transformations. *International Journal of Remote Sensing*, **9**, pp. 187–236.

VERHOEF, W., MENENTI, M. and AZZALI, S., 1996, A colour composite of NOAA-AVHRR-NDVI based on time series analysis (1981–1992). *International Journal of Remote Sensing*, **17**, pp. 231–235.

VERSTRAETE, M.M., PINTY, B. and CURRAN, P.J., 1999, MERIS potential for land applications. *International Journal of Remote Sensing*, **20**, pp. 1747–1756.

WILS, W.P.J., 1994, The Birds Directive 15 Years Later – a Survey of the Case Law and a Comparison with the Habitats Directive. *Journal of Environmental Law*, **6**, pp. 219–242.

ZHAN, X., SOHLBERG, R.A., TOWNSHEND, J.R.G., DIMICELI, C., CARROLL, M.L., EASTMAN, J.C., HANSEN, M.C. and DEFRIES, R.S., 2002, Detection of land cover changes using MODIS 250 m data. *Remote Sensing of Environment*, **83**, pp. 336–350.

ZURITA-MILLA, R., CLEVERS, J.G.P.W., SCHAEPMAN, M.E. and KNEUBUEHLER, M., 2006, Effects of MERIS L1b radiometric calibration on regional land cover mapping and land products. *International Journal of Remote Sensing*, **27**, pp. 653–673.